J. Fluid Mech. (1990), *vol.* 219, *pp.* 195–214
Printed in Great Britain

The decay power law in grid-generated turbulence

By MOHSEN S. MOHAMED† AND JOHN C. LARUE
Department of Mechanical Engineering, University of California, Irvine, CA 92717, USA

(Received 2 October 1989 and in revised form 15 February 1990)

The effect of initial conditions on the decay exponent and coefficient and virtual origin in the decay power-law form for the variation of the variance of the turbulent velocity downstream of biplane grids constructed of rods of both round and square cross-section is determined. This effect is determined for data obtained as part of the present study as well as from previous studies. These studies cover a Reynolds number range from 6000 to 68000, mesh sizes of 2.54 and 5.08 cm, and solidities of 0.34 and 0.44.

It is shown that the choice of the virtual origin and the use of data in the non-homogeneous portion of the flow can have a significant influence on the value of the parameters in the decay power-law. Criteria are developed to identify the nearly homogeneous and isotropic portion of the flow. These criteria include low values of the velocity skewness, constancy of the skewness of the velocity derivative and balance of the turbulent kinetic energy equation.

Results based on data selected by means of these criteria show that the decay exponent and virtual origin are independent of initial conditions such as Reynolds number, mesh size, solidity, and rod shape and surface roughness with values of respectively 1.30 and 0. In contrast and as expected, the decay coefficient is found to be a function of these initial conditions. Thus, the downstream variation of the variance of the turbulent velocity is universally self-similar.

1. Introduction

Starting with the initial studies of Taylor (1935), owing to its relative simplicity and its usefulness as an aid in understanding the fundamental properties of turbulent flows, the study of homogeneous and isotropic turbulence has received widespread attention. Comprehensive reviews are presented by Batchelor (1953), Hinze (1959) and Monin & Yaglom (1975).

In particular, analyses based on the assumption of self preservation or self similarity of the correlation, structure, or spectral functions have led to predictions for the decay of the variance of the downstream component of the fluctuating velocity which have a power-law form (cf. von Kármán & Howarth 1938; Kolmogorov 1941; Saffman 1967; George 1988). Specifically, these predictions for the decay of the velocity variance have the form:

$$\overline{u^2} = a_1(t-t_0)^{-n}, \tag{1}$$

where $\overline{u^2}$ is the variance of the downstream component of the turbulent velocity, a_1

† Present address: The Department of Mechanical Engineering, Faculty of Engineering, Cairo University, Cairo, Egypt.

is a coefficient which depends on initial conditions, t is time, t_0 is the virtual origin, and n is the decay exponent.

In this paper an alternate, but equivalent form of the decay power law is used, which is obtained from (1) by using Taylor's hypothesis to convert from time to downstream position and dividing both sides by U^2 where U is the mean velocity. As a result of these operations, the following form for the power law is found:

$$\overline{u^2}/U^2 = A(x/M_u - x_o/M_u)^{-n} \tag{2}$$

where $A = a_1/(U^{2-n}M_u^n)$ is the decay coefficient, x is the coordinate, positive in the downstream direction with origin at the grid, x_o is the virtual origin, and M_u is the mesh size.

While the analyses of von Kármán & Howarth (1938), Kolmogorov (1941) and Saffman (1967) lead to the same form for the decay of the velocity variance, they do not lead to the same predicted value for the decay exponent. The corresponding predicted values for n are respectively 1, $\frac{10}{7}$ and $\frac{6}{5}$.

In contrast, George (1988) has suggested that there may not be a universal self-preserving state for grid generated flows. More specifically, the decay exponent and coefficient may not be a constant but may vary as a function of initial conditions. A review of various experimental results might appear to support George's suggestion. For example, while Batchelor & Townsend (1947, 1948), Stewart & Townsend (1951) and Portfors & Keffer (1969) find that $n = 1$, Corrsin (1963), Uberoi (1963), Uberoi & Wallis (1967, 1969) and Comte-Bellot & Corrsin (1971) find that $1.16 \leqslant n \leqslant 1.37$. In addition, higher values of n, e.g. 1.43, have been found (cf. Baines & Peterson 1951).

Aside from the possibility that there may not be a universal self-preserving state, one other possible reason for the variation in the values of n and A is that the corresponding data have not been analysed in a consistent manner. For example, in some studies, data near the grid where the flow is inhomogeneous and anisotropic and the power-law decay is inapplicable, is used to determine n. Also, in many studies, the virtual origin is not determined in a consistent and objective manner.

The purpose of the present study is to present an objective method for the determination of the virtual origin, decay exponent, and associated coefficient which is applicable not only to data obtained in the flow downstream of a grid but also, in concept and in modified form, to other self-preserving flows. The approach used in the study discussed herein is to perform a careful analysis relevant to the selection of the virtual origin and selection of data in the power-law region for data obtained as part of the present study. The results of that analysis are next applied to data obtained in a number of previous studies. The comparison of the values for the decay exponent and coefficient and the virtual origin from the present and previous studies is used to determine the effect of initial conditions on those quantities and the lack or presence of universal self-preservation.

In §2 we discuss the relevant characteristics of the flow downstream of biplane grids. The experimental arrangement and techniques for the present study are presented in §3. The results are given in §4 and a summary of the conclusions in §5.

2. Background

In this section a brief review of the relevant characteristics of the flow field downstream of a biplane grid is presented. This is followed by a discussion of criteria that can be used to indicate when the flow is locally isotropic.

The flow field downstream of a biplane grid in a wind tunnel is described in detail

by Monin & Yaglom (1975) and hence only a brief description is presented here. The flow field downstream of a grid can be divided basically into three regions. The first is the developing region nearest the grid where the rod wakes are merging, the flow is inhomogeneous and anisotropic and, consequently, there is production of turbulent kinetic energy. This region is followed by one where the flow is nearly homogeneous, isotropic and locally isotropic but where there is appreciable energy transfer from one wavenumber to another. It is in this region that the form of the power-law decay discussed in this study is applicable. The third region or final period of decay where viscous effects act directly on the large energy containing scales is furthest downstream from the grid (cf. Batchelor 1953).

Since the form of the decay power law discussed herein is applicable only in the second or power-law region, it is important that only data from that region be used to determine the decay exponent and coefficient, and virtual origin. For this reason, studies and criteria which relate to identification of the downstream positions where the decay power-law region begins and ends and, in particular, where the flow becomes nearly homogeneous, isotropic and locally isotropic are next presented.

One of the more detailed studies of the approach to homogeneity in grid generated flows is presented by Grant & Nisbit (1957). They find that the anisotropy and inhomogeneity diminish very slowly with downstream distance from the grid and that the position where the flow becomes homogeneous and isotropic depends on M_u and Re_{M_u}. For example, 80 mesh lengths downstream of a grid with a mesh size of 1.27 cm, they find about a 30% variation in $\overline{u^2}$ in the direction normal to the mean flow direction. They also find that the decay coefficient and exponent obtained along different mean streamlines vary.

In addition, Corrsin (1963) shows that the shape of the grid elements and its solidity ratio have important effects on both the homogeneity, intensity level and the stability of the wake system generated by the grid elements. Also, Uberoi & Wallis (1967) show that the homogeneity, even as far downstream as $x/M_u = 95$, depends on the accuracy of the grid construction and the surface roughness of the grid-rod elements. Further, Corrsin (1963) shows that 'an effective homogeneity' is generally attained when $\mathrm{d}L_x/\mathrm{d}x \ll 1$; $(L_x/\lambda)(\mathrm{d}\lambda/\mathrm{d}x) \ll 1$; and $(-L_x/u^2)(\mathrm{d}\overline{u^2}/\mathrm{d}x) \ll 1$, where L_x and λ are respectively the integral and Taylor lengthscales. For grids with a relatively low solidity, such as the ones considered in this study, Corrsin (1963) suggests that these conditions are satisfied at $x/M_u \geqslant 40$.

The skewness of the velocity, $S(u) = \overline{u^3}/\overline{u^2}^{\frac{3}{2}}$, provides one means to assess the approach to isotropy of the flow. Based on simple arguments concerning reflection of the downstream coordinate axis, the velocity skewness should be zero in an isotropic flow.

One indicator of the position where the flow becomes locally isotropic is based on the analysis of Batchelor (1953) who shows that, in a flow that is both locally isotropic and locally similar, the skewness of the velocity derivative, $S(\partial u/\partial x) = \overline{(\partial u/\partial x)^3}/(\overline{(\partial u/\partial x)^2})^{\frac{3}{2}}$, should be a constant. Thus, the position in the flow where $S(\partial u/\partial x)$ becomes a constant can be taken as the position where the flow becomes locally isotropic.

A second indicator of the position where the flow becomes locally isotropic is provided by a comparison of the dissipation rate of turbulent kinetic energy computed from the balance equation to that computed from the variance of the velocity derivative.

The three criteria discussed in the preceding, the criteria of Corrsin (1963), and measurements of statistical properties of the flow in the transverse direction are all

M_u (cm)	Re_{M_u}	$Re_\lambda{}^a$	λ^a	$L/M_u{}^a$
2.54	6000	28.37	0.639	0.476
2.54	10000	36.07	0.497	0.471
2.54	14000	41.60	0.423	0.467
5.08	12000	43.85	0.920	0.529

[a] Evaluated at $x/M_u = 40$.

TABLE 1. Flow parameters

used in the present study to determine the downstream position where the flow becomes nearly isotropic, homogeneous and locally isotropic.

3. Experimental arrangement and techniques

Results obtained as part of the study discussed herein are obtained in the UCI Wind Tunnel which has a test section with a cross-section of 0.91×0.61 m and a length of 6.71 m. The tunnel is operated in a closed return mode and has a measured free-stream turbulence intensity of less than 0.1 % in the velocity range 3–12 m/s. The turbulence generator is one of two biplane grids constructed of polished aluminium rods. The rod diameters are 0.476 or 0.95 cm with corresponding mesh sizes of 2.54 and 5.08 cm. The two grids have the same solidity ratio of 0.34 and are placed 0.9 m downstream of the exit of the contraction. The mean velocity in the tunnel is monitored by means of a MKS Baratron pressure transducer connected to a Pitot-static tube.

A hot-wire sensor, operated in the constant temperature mode by means of a TSI Model 1050A anemometer, is used to measure the time resolved axial velocity fluctuations. The wire is oriented horizontally in a direction normal to the mean flow. The wire is made from platinum-plated tungsten and is 5.0 μm in diameter and 1.25 mm in length. Based on the square-wave test, the hot wire is found to have a frequency response in excess of 20 kHz in the velocity range of interest. An analogue, electronic differentiator is used to obtain the time derivative of the velocity.

The hot wire and its derivative signal are conditioned using precision buck and gain amplifiers and subsequently low-pass filtered at 3 kHz. The signals are recorded on analogue magnetic tape at a tape speed of 38.1 cm/s which corresponds to a frequency response of 5 kHz. The recorded signals are played back and digitized at a sample rate of 6000 samples/s. The digitized signals which correspond to 35 s of real time at each point, are stored on digital magnetic tape and then analysed on a digital computer using standard analysis software.

The downstream decay data are collected along the centreline of the tunnel while data used to assess the transverse homogeneity are collected in the transverse direction at different downstream positions. The Reynolds numbers and other relevant flow parameters are shown in table 1.

4. Experimental results and discussion

The approach of the present flow to one that is nearly homogeneous is first discussed. This is followed by a discussion of criteria used to assess the isotropy and local isotropy of the flow.

Subsequently, the effect of variation of the virtual origin on the decay coefficient

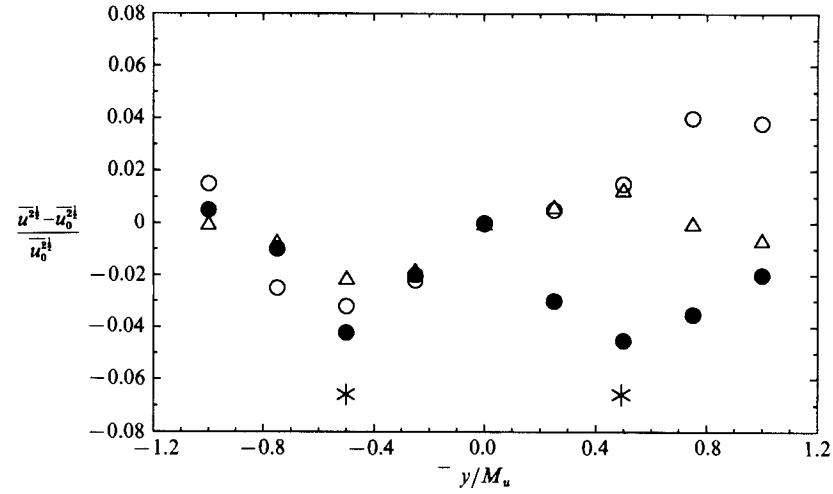

FIGURE 1. Transverse variation of the difference of the root mean square of the downstream turbulent velocity, $\overline{u^2}^{\frac{1}{2}}$, and the centreline value normalized by the centreline value, $\overline{u_0^2}^{\frac{1}{2}}$; ○, $Re_{M_u} = 14000$, $x/M_u = 11$; ●, $Re_{M_u} = 6000$, $x/M_u = 40$; △, $Re_{M_u} = 14000$, $x/M_u = 40$; and, *, corresponds to the position of the horizontal grid rods nearest the centreplane.

and exponent and methods used to select the virtual origin are discussed. In the final subsection, the decay coefficient and exponent obtained in both the present and previous studies are compared to the values obtained using data from those same studies but where only data in the nearly homogeneous and isotropic, decay power-law portion of the flow are used and where the virtual origin is chosen in a consistent manner for all data sets.

4.1. *Homogeneity, isotropy and local isotropy*

In this subsection, the approach of the flow to one that is homogeneous in a transverse plane is first discussed. Next, criteria used to assess the isotropy and local isotropy of the flow are discussed.

4.1.1. *Homogeneity*

The transverse variation of the difference between the root-mean-square longitudinal velocity and that at the centreline is shown in figure 1. The minima and maxima in the profiles correspond to the positions of the grid rods which are indicated by the * shown at $y/M_u = -0.5$ and 0.5 where y is the transverse coordinate with origin at the centreline.

As expected, the transverse variation in the r.m.s. downstream velocity is found to decrease in the downstream direction. For example, at $x/M_u = 11$ for $Re_{M_u} = 14000$, the peak to peak variation is about 7% and decreases to less than 3% at $x/M_u = 40$. For $Re_{M_u} = 6000$ and $x/M_u = 11$, the peak to peak variation is about 4%. This is slightly more than half the variation found at the higher Reynolds number. This reduced variation at the lower Reynolds number indicates that the flow will become nearly homogeneous closer to the grid than at higher Reynolds numbers. These observations are in agreement with the corresponding results of Grant & Nisbet (1957).

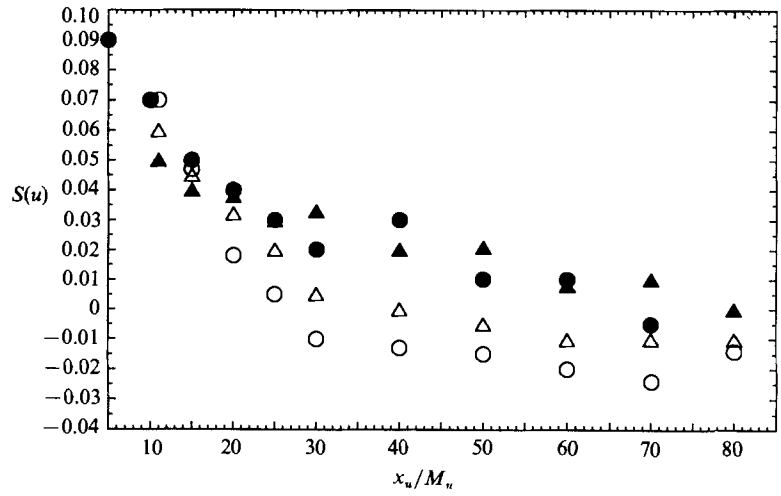

FIGURE 2. Effect of Re_{M_u} and M_u on the downstream variation of the velocity skewness, $S(u)$. See table 2 for symbols.

4.1.2. *Isotropy*

In an isotropic flow, the skewness of the velocity, $S(u) = \overline{u^3}/\overline{u^2}^{\frac{3}{2}}$, has zero value. Thus, the value of $S(u)$ as a function of downstream position, which is shown on figure 2 (see also table 2), provides one means to assess the approach of the flow to an isotropic condition. Near the grid where the flow is neither homogeneous nor isotropic, the value of the velocity skewness for $Re = 6000$, 10000, and 14000 and $M_u = 2.54$ cm and for $Re = 12000$ and $M_u = 5.08$ cm are small but positive. All values decrease with increasing downstream distance and values for the two lower Reynolds number values are seen to asymptotically approach values of, respectively, about -0.015 and -0.010. At a fixed downstream position, $S(u)$ is seen to increase with increasing Reynolds number.

The positive values of $S(u)$ near the grid and decreasing values with increasing downstream distance and decreasing Reynolds numbers are not inconsistent with the corresponding measurements of Bennett & Corrsin (1978) and analysis of Maxey (1987). In his analysis, Maxey considers the velocity skewness to be the downstream flux of turbulent kinetic energy which he shows to be proportional to $\overline{u^2}$. Thus, consistent with the present measurements, $S(u)$ would be expected to be initially positive and to decrease in magnitude with increasing downstream distance.

However, it should be noted that, as indicated in figure 1, the initially positive and subsequently decreasing values of $S(u)$ correspond to the inhomogeneous region of the flow. Thus, the positive values of $S(u)$ may be due, at least partially, to the occasional passage of a fluid particle from a portion of the flow where the turbulent kinetic energy is relatively higher. Additional measurements of $S(u)$ in the transverse direction would be useful in assessing the effect of inhomogeneity.

The negative values of $S(u)$ for $Re = 6000$ and 10000 which start, respectively, at about $x/M_u = 29$ and 39 are not inconsistent with the measurements of Bennett & Corrsin (1978) but are with the analysis of Maxey (1987). However, the uncertainty of the data appears to be about ± 0.01 which is about the same as the uncertainty estimate of Helland & Stegan (1970). Thus, the small negative values must be interpreted with some caution and may not be inconsistent with the analysis of Maxey (1987) but rather may be due to the uncertainty of the data.

Reference	No.[a]	Sym.[b]	Re_{M_u} $\times 10^{-3}$	M_u cm	σ	n_{old}[c]	A_{old}[c] $\times 10^4$	x_o/M_u[c]	n[d]	A[d] $\times 10^4$
Present results[e]	1	○	6.00	2.54	0.34	1.472	798.0	0	1.309	435.5
		△	10.0	2.54	0.34	1.463	727.8	0	1.309	424.6
		▲	14.0	2.54	0.34	1.421	786.1	0	1.285	364.0
		●	12.0	5.08	0.34	1.463	916.2	0	1.299	490.9
Kanellopoulos (private communication, 1987)	2	◪	13.5	2.50	0.35	1.360	—	—	1.289	379.3
Batchelor & Townsend (1948)[e]	3		5.50	1.27	0.34	1.000	132.0	12.0	1.185	201.0
			11.0	1.27	0.34	1.000	151.0	15.0	1.316	327.0
Wyatt (1955)	4	◪	11.0	2.54	0.34	1.270	322.0	5.0	1.330	495.0
		◔	22.0	2.54	0.34	1.270	285.7	3.5	1.318	381.9
			44.0	5.08	0.34	1.250	285.7	4.0	1.31	398.1
Van Atta & Chen (1969)	5	◇	25.6	2.54	0.34	—	—	—	1.304	364.8
		◆	25.3	5.08	0.34	—	—	—	1.330	414.0
Comte-Bellot & Corrsin (1966)	6		34.0	5.08	0.44	1.300	434.8	2.0	1.331	515.3
			68.0	5.08	0.44	1.270	370.4	2.0	1.299	434.5
Sreenivasan *et al.* (1980)[d]	7		7.40	2.54	0.44	1.200	400.0	3.0	1.243	505.8
Uberoi (1963)[e]	8		29.0	2.54	0.44	1.200	—	—	1.257	571.5
Uberoi & Wallis (1967)[e] (wooden rods)	9	⊕	8.75	2.54	0.34	1.310	—	—	1.303	642.7
			17.5	5.08	0.34	1.240	—	—	1.295	433.5
			17.5	5.08	0.44	1.280	—	—	1.305	481.9
Sirivat & Warhaft (1983)[f]	10	□	5.15	2.54	0.34	1.290	664.0	0	1.290	664.0
			9.55	2.54	0.34	1.370	1051.0	0	1.370	1051.0

[a] The number in this column corresponds to the number used to identify the data source on figures 11 and 12.
[b] The indicated symbols are those used in figures 2–4 and 7–10.
[c] The values for n_{old}, A_{old}, and x_o/M_u are those presented in the corresponding reference.
[d] The values for n and A are obtained in the present study using a value of zero for the virtual origin.
[e] Data from both the inhomogeneous and homogeneous portions of the flow have been used to determine n_{old} and A_{old}.
[f] These results are obtained for a grid composed of rods of square cross-section.

TABLE 2. The decay power-law exponent and coefficient for the present and previous results

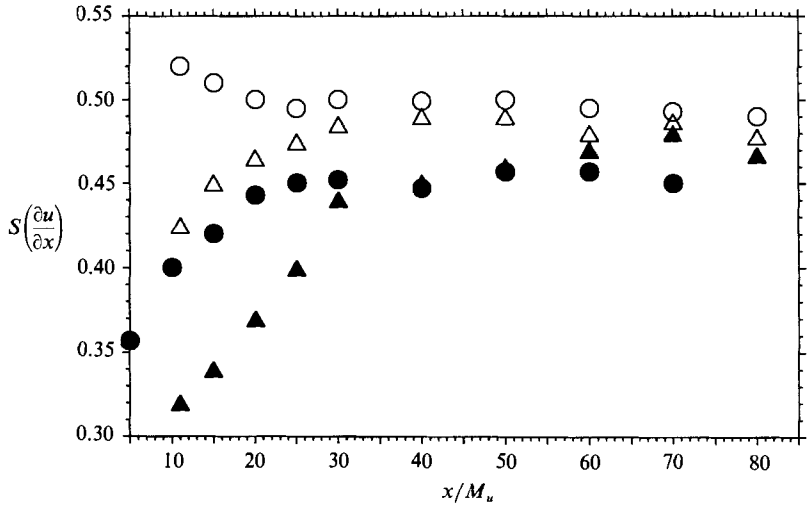

FIGURE 3. Effect of Re_{M_u} and M_u on the downstream variation of the skewness of the velocity derivative, $S(\partial u/\partial x)$. See table 2 for symbols.

Corresponding to the uncertainty of ± 0.01, the position where $S(u) = 0.01$ is taken to be that where the flow becomes isotropic. The corresponding positions in ascending magnitude of Reynolds number are $x/M_u = 24$, 30, 45, and 55.

4.1.3. *Local isotropy*

Considered first as an indicator of the position where the flow becomes locally isotropic is the variation of $S(\partial u/\partial x)$ with downstream position which is shown on figure 3. It can be seen that the value of $S(\partial u/\partial x)$ approaches a constant which has a value that depends on Re_λ. The value is seen to decrease with increasing Re_λ. For example, for an increase in Re_λ from 28.4 to 43.9, the value of $S(\partial u/\partial x)$ decreases from about 0.5 to 0.45. These results are consistent with the corresponding results of Stewart & Townsend (1951) and Frenkiel & Klebanoff (1971), and the predictions of McComb, Shanmugasundaram & Hutchinson (1990). The downstream position where the nearly constant value of $S(\partial u/\partial x)$ is reached appears to correlate well with Re_{M_u} and is seen to increase from $x/M_u = 25$ to 55 as Re_{M_u} increases from 6000 to 14000.

Local isotropy of the flow can also be assessed by comparing the dissipation rate computed using the appropriate form of the turbulent kinetic energy equation and that computed using the velocity time derivative. In the nearly homogeneous and isotropic region downstream of the grid the turbulent kinetic energy equation becomes (cf. Comte-Bellot & Corrsin 1966)

$$\epsilon_u^* = -\frac{1}{2}\frac{\mathrm{d}\overline{q^2}}{\mathrm{d}t}, \tag{3}$$

where $\overline{q^2} = (\overline{u^2} + \overline{v^2} + \overline{w^2})$.

Using Taylor's hypothesis and the assumptions of isotropy and homogeneity in the decay power-law region (i.e. $\overline{u^2} \approx \overline{v^2} \approx \overline{w^2}$), the above expression can be written as:

$$\epsilon_u^* = -\tfrac{3}{2}U\frac{\mathrm{d}\overline{u^2}}{\mathrm{d}x}. \tag{4}$$

The value of $\mathrm{d}\overline{u^2}/\mathrm{d}x$ can be computed directly from the data for $\overline{u^2}$ versus x/M_u. Near the grid, owing to the anisotropy and inhomogeneity, it is expected that this form of

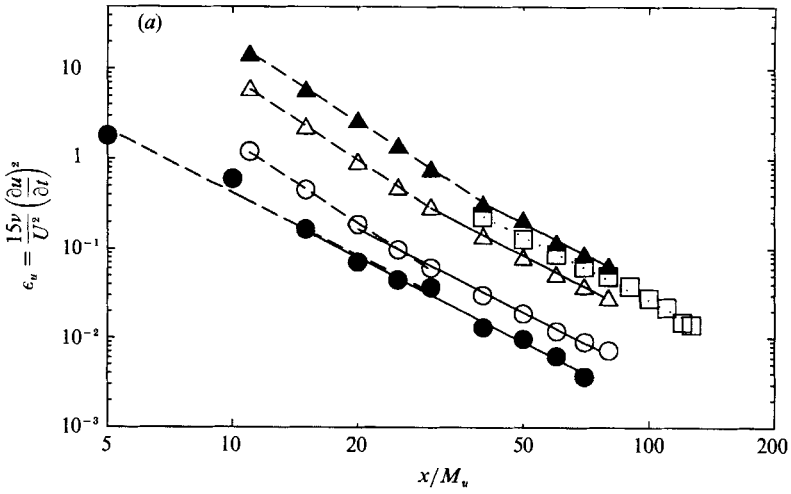

FIGURE 4. Variation of the dissipation rate of turbulent kinetic energy computed as: $\epsilon_u = (15\nu/U^2)\,\overline{(\partial u/\partial t)^2}$. See table 2 for symbols.

the turbulent kinetic energy equation will yield inaccurate estimates of the dissipation rate.

A second and independent estimate of the dissipation rate, ϵ_u, is obtained using the measured time derivative of the downstream velocity, Taylor's hypothesis and the assumption of local isotropy. The corresponding expression for the dissipation rate is as follows:

$$\epsilon_u = \frac{15\nu}{U^2}\overline{\left(\frac{\partial u}{\partial t}\right)^2}. \tag{5}$$

Since the flow is not locally isotropic near the grid, this estimate for the dissipation rate is expected to be in error near the grid.

While the expression for ϵ_u is based on the assumption of local isotropy, the expression for ϵ_u^* is based on both the assumptions of homogeneity and isotropy. At downstream distances far enough from the grid, where the flow is nearly homogeneous, isotropic and locally isotropic, the ratio, ϵ_u/ϵ_u^* should be nearly unity.

The results shown on figure 4 are for the dissipation rate, ϵ_u, computed using the velocity derivative for the present data and also for the data of Sirivat & Warhaft (1983) who use a square-rod grid. These results show that, near the grid, ϵ_u decays faster than it does further downstream. The extent of the region of faster decay is seen to increase as the Reynolds number is increased and as the grid mesh size is decreased. For corresponding values of Re_{M_u}, the positions where the rate of decrease of ϵ_u changes is approximately the same as the positions where $S(\partial u/\partial x)$ becomes a constant.

The downstream variation of the dissipation rate computed using the turbulence kinetic energy equation is shown on figure 5. Along with the present results, the corresponding results from Comte-Bellot & Corrsin (1971), Sirivat & Warhaft (1983) and Kanellopoulos (private communication, 1987) are also presented. The slopes for the different data sets are in general agreement and vary from -2.36 to -2.47. For all the data sets, there is no indication of a change in the rate of decrease of ϵ_u^* with downstream position.

Figure 6 shows the ratio, ϵ_u/ϵ_u^*, for the present results and those of Sirivat & Warhaft (1983). The ratio, ϵ_u/ϵ_u^*, differs significantly from unity in the initial region

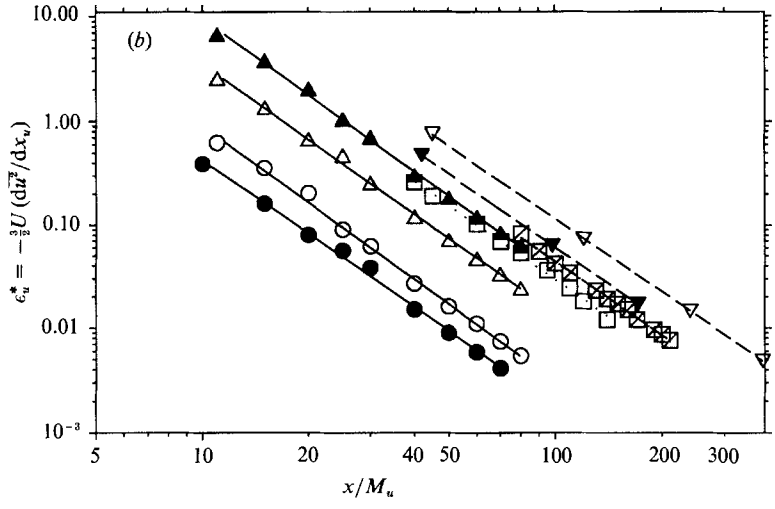

FIGURE 5. Variation of the dissipation rate of turbulent kinetic energy computed as: $\epsilon_u^* = -\frac{3}{2}U(\mathrm{d}\overline{u^2}/\mathrm{d}x)$. See table 2 for symbols.

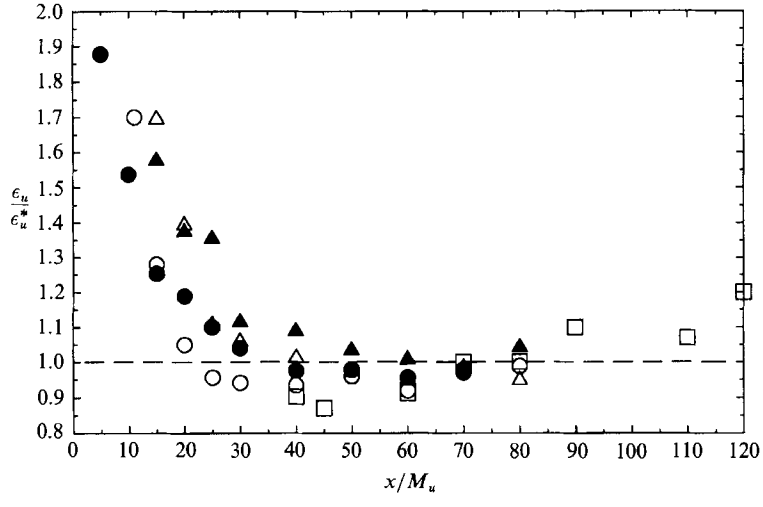

FIGURE 6. Ratio of the dissipation rate of the turbulent kinetic energy, ϵ_u/ϵ_u^*. See table 2 for symbols.

near the grid where a relatively high degree of anisotropy and inhomogeneity is expected. However, a value of unity is approached at downstream positions which vary from $x/M_u = 25$ to 55. For corresponding values of the Reynolds number, the position where the value of unity is reached is about the same as that where a constant value for $S(\partial u/\partial x)$ begins. It should be noted that the present observations are in general agreement with those of Sirivat & Warhaft (1983).

In summary, the results shown in figures 1–3 and 6 indicate that the flow becomes nearly locally isotropic, isotropic and homogeneous starting at about x/M_u equal to 25, 40, 50 and 55 for respectively $Re_{M_u} = 6000$, 10000, 12000, and 14000. For the present data, these positions are taken to correspond to the beginning of the decay power-law region. For previous data sets, this position, consistent with the suggestion of Corrsin (1963), is taken to be $x/M_u = 40$. Consequently, results from previous

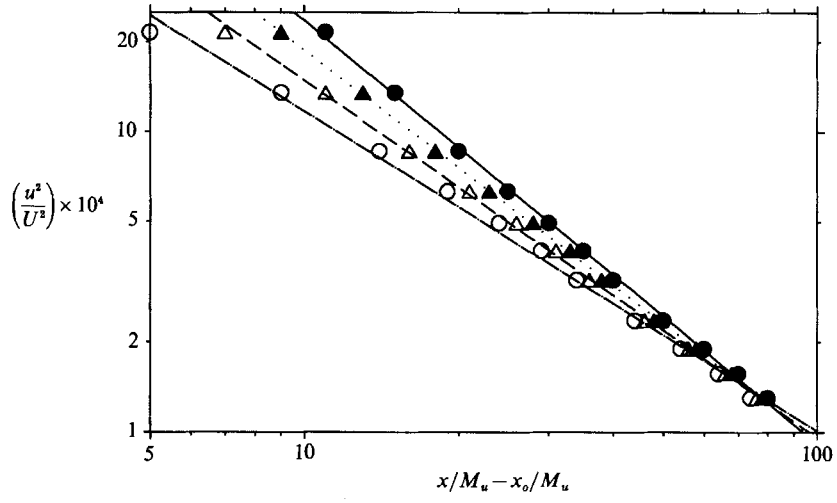

FIGURE 7. Decay of the normalized variance of the downstream turbulent velocity using different values for the virtual origin for $Re_{M_u} = 14000$ and $M_u = 2.54$ cm. Symbols correspond to measured values while lines correspond to the decay-law equation obtained by applying the method of least squares to the corresponding data with $x/M_u - x_o/M_u$ as the independent variable; ○, $x_o/M_u = 0$; △, $x_o/M_u = 2$; ▲, $x_o/M_u = 4$; ●, $x_o/M_u = 6$. (Corresponding values of the decay exponent, coefficient, and standard error may be found in table 3.)

studies at Reynolds numbers higher than 10000 may be based on a limited amount of data obtained in portions of the flow that are inhomogeneous and anisotropic. Since only a few data points might be obtained in the inhomogeneous and anisotropic portion of the flow the effect on the values of the virtual origin and decay coefficient and exponent should be negligible.

The observed increase in the downstream position with increasing Reynolds number where the flow becomes nearly isotropic and locally isotropic is related to the characteristic timescale of the large-scale structure. This assertion is based on the assumption that the time required for the large-scale anisotropic structures to decay and become isotropic is proportional to the characteristic time, τ, of the large-scale structure. Tennekes & Lumley (1989) suggest that the characteristic time of the large-scale structures is proportional to the convection time which in turn is taken equal to x/U. Thus,

$$\tau = C\frac{x}{U}, \tag{6}$$

which C is the constant of proportionality.

Consequently, for a constant mesh size, consistent with the observations, the position corresponding to the characteristic timescale is proportional to the Reynolds number and is expected to increase with increasing Reynolds number. Thus, the ratio of the positions where the flow becomes isotropic should be equal to the ratio of the corresponding Reynolds numbers. For pairs of Reynolds numbers of 6000 and 10000 and also 6000 and 14000, the Reynolds number ratios are, respectively 1.66 and 2.33. The corresponding ratio of the approximate positions where the flow becomes isotropic are, respectively, 1.6 and 2.2. The similarity of the values of the corresponding ratios is supportive of the proposed explanation.

For grids of two different mesh sizes with the same mean velocity, the position where the flow becomes isotropic would be expected to be the same. The mean

x_o/M_u	n	Std. err. $\times 10^4$	A $\times 10^4$
0	1.42	0.164	786.1
2	1.33	0.184	374.3
4	1.10	0.252	182.6
6	0.95	0.268	91.33

TABLE 3. Decay exponent, coefficient, and standard error for four different values of the virtual origin for $M_u = 2.54$ cm and $Re_{M_u} = 14000$ using data in both the inhomogeneous and anisotropic and nearly homogeneous and isotropic portions of the flow

velocity is 3.66 m/s for both $M_u = 2.54$ cm and $Re = 6000$ and also $M_u = 5.08$ cm and $Re = 12000$. However, the corresponding positions where the flow becomes nearly isotropic and locally isotropic are found to be about $x/M_u = 25$ and 50. In physical units, the position where isotropy is reached for the grid with $M_u = 5.08$ cm is a factor of four larger than for the grid with $M_u = 2.54$ cm. The reason for this inconsistency is not obvious.

4.2. *Determination of the virtual origin*

The power-law expression contains three unknown constants, A, n and x_o, which must be determined. The virtual origin, x_o, is used to account for the fact that the effective origin of the turbulent velocity fluctuations may not coincide with the location of the grid. Typical values for the virtual origin fall in the range of 0 to 20 (cf. Batchelor & Townsend 1948; Comte-Bellot & Corrsin 1966).

As shown on figure 7, the value of the virtual origin, even for the limited range of 0–6, can have a significant effect on the decay exponent. For example, this variation in value of the virtual origin, as shown in table 3, leads to a change in the decay exponent from 1.42 to 0.95 and a change in the decay coefficient from 786.1 to 91.33. Here it should be noted that data used to obtain these results correspond to both the inhomogeneous and homogeneous portions of the flow and that exponents less than 1 would correspond to an increase in turbulent kinetic energy with downstream distance and hence can be rejected on physical grounds.

Qualitatively similar results are obtained when only data obtained in the nearly homogeneous portion of the flow are used. There are, however, quantitative differences. For example, use of data only in the nearly homogeneous and isotropic portion of the flow and a virtual origin of zero leads to a decay exponent and coefficient of respectively 1.285 and 364.0. Thus, there is a reduction in the decay exponent and coefficient of respectively 9% and more than 50%. Therefore, it seems clear that objective criteria must be used to choose only data in the nearly homogeneous and isotropic portion of the flow. In addition, the method used to determine the virtual origin must be objective and accurate.

The decay exponent and coefficient which correspond to the selected values for the virtual origin indicated on figure 7 and which are used in the subsequent analysis are determined using a procedure based on one used by Comte-Bellot & Corrsin (1966) and Sreenivasan, Tavoularis & Corrsin (1980). There, the decay power-law expression (equation (2)) is rewritten as:

$$\log(\overline{u^2}/U^2) = \log(A) - (n)\log(x/M_u - x_o/M_u). \tag{7}$$

A value for x_o/M_u is assumed and the method of least squares is used to obtain the corresponding values for A and n.

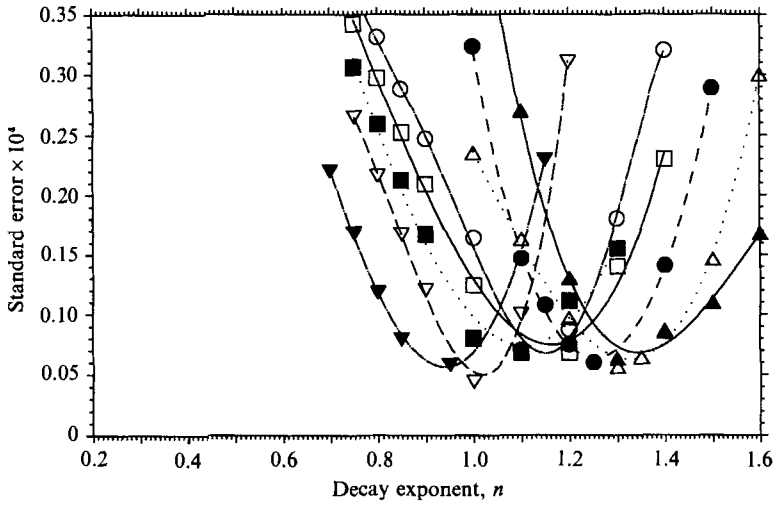

FIGURE 8. Variation of the standard error as a function of the decay exponent for different values for the virtual origin for $Re_{M_u} = 14000$ and $M_u = 2.54$ cm; ▲, $x_0/M_u = 0$; △, $x_0/M_u = 2$; ●, $x_0/M_u = 4$; ○, $x_0/M_u = 6$; □, $x_0/M_u = 8$; ■, $x_0/M_u = 10$; ▽, $x_0/M_u = 12$; ▼, $x_0/M_u = 14$. The corresponding values of the decay exponent and coefficient, n_{opt} and A_{opt}, which correspond to the minimum standard error for each value of the virtual origin are shown in table 4. (Lines are shown only to aid in observing the trend of the data.)

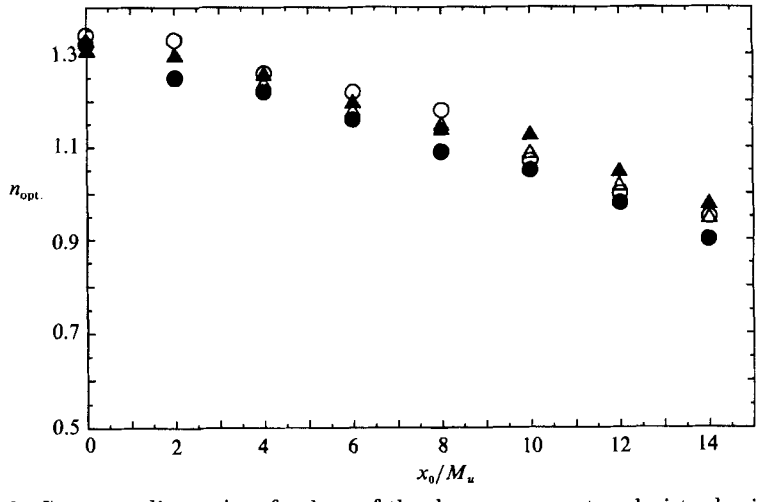

FIGURE 9. Corresponding pairs of values of the decay exponent and virtual origin that lead to a relative minimum of the standard error. See table 2 for symbols.

These corresponding values for A and n are the ones that lead to a minimum for the root mean square of the difference between corresponding values of measured and computed values of $\overline{u^2}/U^2$. Unfortunately, values for the root mean square of the difference, hereinafter referred to as the standard error, do not differ significantly for the different values of x_0/M_u. Thus, use of the method of least squares or a similar method to determine the virtual origin and corresponding decay coefficient and exponent will not yield unambiguous results.

The results shown on figure 8 illustrate this point. There the standard error is shown plotted as a function of the decay exponent for different values of the virtual

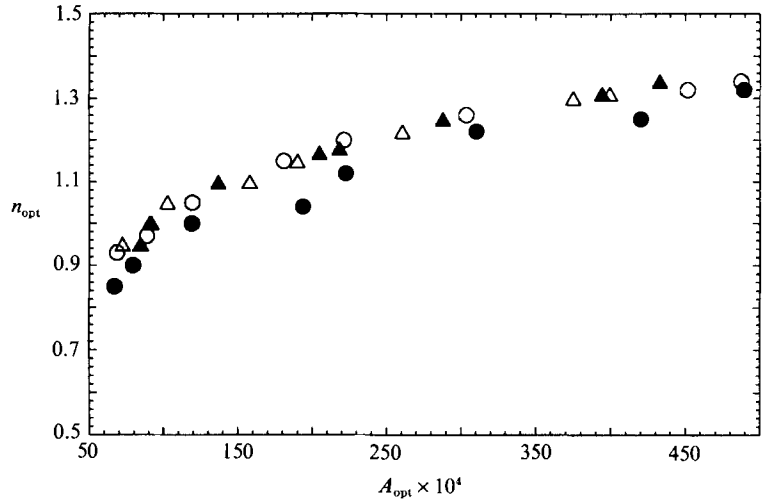

FIGURE 10. Corresponding pairs of values of the decay exponent and coefficient that lead to a relative minimum of the standard error. See table 2 for symbols.

x_o/M_u	n_{opt}	$A_{opt} \times 10^4$
0	1.31	394.1
2	1.34	432.7
4	1.25	288.2
6	1.18	218.4
8	1.17	205.1
10	1.10	136.7
12	1.00	90.68
14	0.95	84.46

TABLE 4. Optimized decay exponent and coefficient for different values of the virtual origin for $M_u = 2.54$ cm and $Re_{M_u} = 14000$ using only data from the nearly homogeneous and isotropic portion of the flow

origin. The minima in each of the curves correspond to the exponent, n_{opt}, (and corresponding decay coefficient, A_{opt}) that minimize the standard error for a particular value of the virtual origin. The minimum value for the standard error is seen to be about the same for the eight values of the virtual origin considered. In this figure, only data from the homogeneous portion of the flow are used. Similar results are found for the other data sets of the present study where $Re_{M_u} = 6000$, 10000 and 12000.

The values of n_{opt} as a function of the virtual origin are shown on figure 9. The variation of the virtual origin from 0 to 14, is seen to lead to approximately a 28% variation in n_{opt} with values ranging from about 1.3 to 0.95 (table 4). Except at $x_o/M_u = 0$, the values of n_{opt} for $M_u = 5.08$ cm appear to be consistently lower than the corresponding values for $M_u = 2.54$ cm.

The values of n_{opt} and A_{opt} which correspond to the minima of the standard error for all four Reynolds numbers are shown on figure 10. The optimum decay coefficient, A_{opt}, varies by 79% from 0.0394 to 0.0084. Except at $n_{opt} = 1.3$, for a fixed value of n_{opt}, A_{opt} appears to depend on M_u.

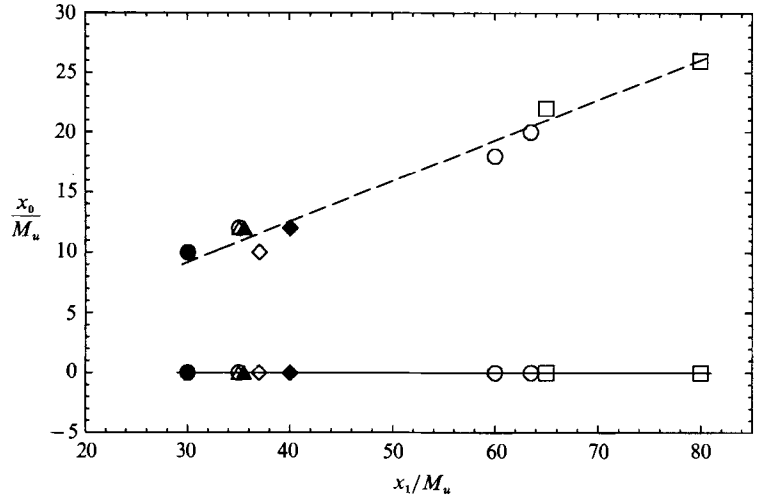

FIGURE 11. Variation of the normalized virtual origin, x_o/M_u as a function of the starting position, x_1/M_u, for $n = 1$ and 1.3. See table 2 for symbols.

Since the standard error associated with each of the corresponding values of n_{opt}, A_{opt}, and x_o/M_u is nearly the same, an additional criteria must be developed which will provide a means to choose a particular set of values. One criteria that can be used to make this choice is based on the assumption that n, A, and x_o/M_u should not depend on the starting position where the data are obtained as long as all the data are obtained in the decay power-law region. The results shown in figure 11 illustrate the application of this criteria.

Shown on that figure are values of the virtual origin which lead to a minimum in the standard error for two fixed values of the decay exponent ($n = 1.0$ and 1.3) as a function of different starting positions, x_1/M_u. The results shown on figure 11 correspond to the present data and those of Van Atta & Chen (1969), Uberoi & Wallis (1967), Wyatt (1955) and Kanellopoulos (private communication, 1987) (the flow conditions corresponding to each study are listed in table 2). For $n = 1$, the virtual origin is seen to increase with increasing starting position. This variation in the virtual origin indicates that $n = 1$ is not the appropriate choice for the decay exponent. However, the nearly constant value of the virtual origin as a function of starting position for $n = 1.3$ indicates that a value of zero is the appropriate choice for the virtual origin.

4.2.1. *Effect of initial conditions on the decay power-law exponent and coefficient*

In this section, the influence of initial conditions such as Re_{M_u}, M_u, grid solidity, σ, and rod shape and surface roughness on the values of the decay coefficient and exponent are assessed. This assessment is applied both to results from the present study and results from previous studies. References for the previous studies along with the Reynolds number and relevant characteristics of the grids are indicated in table 2. Also presented in that table are the values for the decay exponent, decay coefficient, and virtual origin obtained as part of the previous studies. These values are indicated in table 2 respectively by the column headings n_{old}, A_{old}, and x_o/M_u.

Revised values of the decay exponent and virtual origin, indicated respectively by the column headings, n and A, are computed using the data from the previous studies

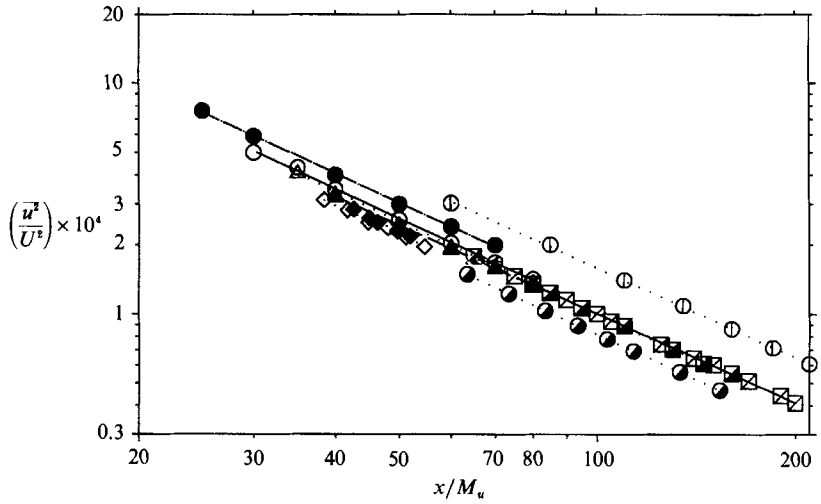

FIGURE 12. Downstream variation of the normalized turbulent velocity variance with a virtual origin of zero. See table 2 for symbols.

but where data at $x/M_u \leqslant 40$ are eliminated from the analysis. In addition, the virtual origin is taken to be zero and the decay exponent and coefficient are found using the method of least squares as described previously.

The more quantitative portion of the analysis relates to results obtained from biplane grids fabricated from smooth, round rods, for two values of the mesh size, 2.54 and 5.08 cm, and two values of the grid solidity, 0.34 and 0.44. Selection of results with these parameters is due to the fact that there appears to be a larger number of results for these conditions than for other conditions. This larger data set leads to a more definitive analysis of the effect of these initial conditions on the decay coefficient and exponent than could be obtained for other initial conditions. However, as indicated in table 2, results for other values of M_u, σ, and rod shape and surface roughness are included for purposes of comparison.

The downstream variation of $\overline{u^2}/U^2$ as a function of x/M_u is shown on figure 12 for grids fabricated from rods of circular cross-section with $\sigma = 0.34$. The line passing through each data set is obtained using the method of least squares. Comparison of this line to the trend of the data indicates the linearity of the data when plotted as a function of x/M_u. Also noteworthy is the observation, that the rough wooden grid rods, as indicated by Uberoi & Wallis (1967), apparently lead to higher values of the relative velocity variance, and hence, a higher value for the decay coefficient, than for smooth rod grids at the same downstream positions.

The decay exponent is shown plotted as a function of Reynolds number in figure 13 for results which correspond to $\sigma = 0.34$ and 0.44 and $M_u = 2.54$ and 5.08 cm. The Reynolds number varies from 6000 to 68000. The mean and root-mean-square values for the decay exponents shown on this figure are respectively 1.300 and 0.024. While there is some scatter in the values for n, it seems clear that there is no systematic variation with Reynolds number, solidity, mesh size or surface roughness.

The decay exponent can also be determined using the measured variation of the dissipation rate as a function of downstream distance as shown in figure 4. It is easy to show, using the turbulent kinetic energy equation and the power-law form for the variation of $\overline{u^2}$, that the variation of the dissipation rate with downstream position is also described by a power-law with an exponent of $-n-1$.

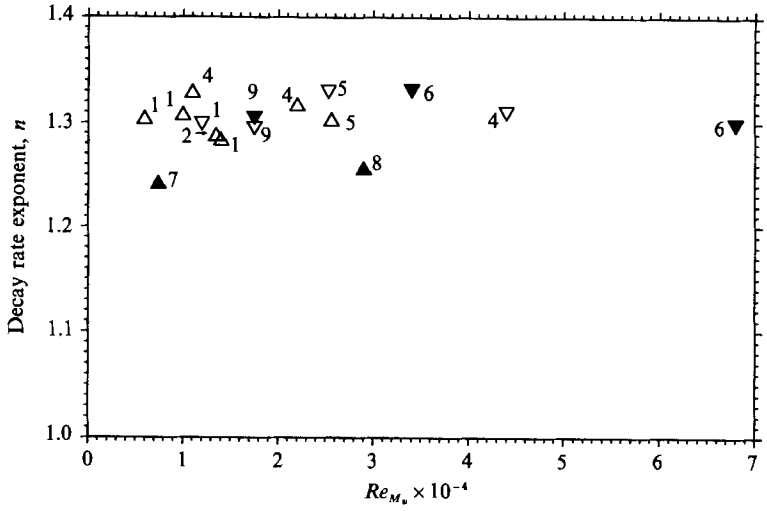

FIGURE 13. Variation of the decay exponent as a function of Reynolds number for $M_u = 2.54$ and 5.08 cm and solidities of 0.34 and 0.44; △, $M_u = 2.54$ cm and $\sigma = 0.34$; ▽, $M_u = 5.08$ cm and $\sigma = 0.34$; ▲, $M_u = 2.54$ cm and $\sigma = 0.44$; and, ▼, $M_u = 5.08$ cm and $\sigma = 0.44$. (Numbers beside symbols refers to the reference numbers in table 2.)

For the present data, in the region where the flow is nearly homogeneous and isotropic, the average value for the exponent in the power-law variation of the dissipation rate is 2.366. The root-mean-square value for the variation of the exponent is 0.0152. Thus, the value of the decay exponent obtained using the dissipation rate exponent is 1.366 which is about 5% higher than the average value found directly from the decay of $\overline{u^2}$. This difference may be due in part to the slight anisotropy and inhomogeneity of the flow but is small enough to be due solely to uncertainty in the measurements.

It should be noted that the values of the decay exponents from Sreenivasan *et al.* (1980) and Uberoi (1963) differ from the mean by about twice the value of the root mean square. These two values correspond to the largest deviation from the mean value but are still relatively small. Since the variation is small, it seems unlikely that the low values are an indication of any systematic variation at low values of the Reynolds number owing to the solidity variation from 0.34 to 0.44.

However as indicated on figure 10, these lower values for the exponent should lead to a smaller value for the decay coefficient than would be found if the exponent were larger. Also of interest is that the rough surface of the grid used by Uberoi & Wallis (1967) appears to have no effect on the decay exponent while it does lead to an increase in the value of the decay coefficient.

Thus, it appears that the decay exponent is not a function of Reynolds number, grid surface roughness, solidity and mesh size for $\sigma = 0.34$ and 0.44 and $M_u = 2.54$ and 5.08 cm in the Reynolds number range from 6000 to 68000. However, extension of these conclusions to round rod grids with smaller mesh size, i.e. $M_u = 1.27$ cm, is not straightforward.

For example, for $M_u = 1.27$ cm, the data of Batchelor & Townsend (1948) lead to the values of n, shown in table 2, of 1.185 and 1.316. The higher value of n which corresponds to a Reynolds number of 11000 is consistent with the preceding observations concerning the invariance of n. However, the lower value which corresponds to a Reynolds number of 5500 falls outside the uncertainty range and

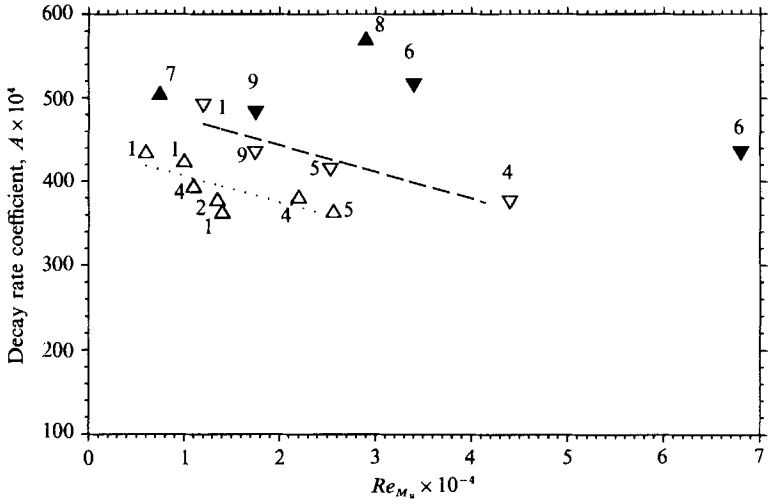

FIGURE 14. Variation of the decay coefficient as a function of Reynolds number for $M_u = 2.54$ and 5.08 cm and solidities of 0.34 and 0.44. Same symbols as for figure 13.

may be indicative of a variation of n with Re_{M_u} for small M_u. In contrast, values for the decay exponent obtained using the square rod data of Sirivat & Warhaft (1983) indicate that grid rod shape has at most a small effect on the decay exponent.

The corresponding decay coefficients, A, are shown plotted as a function of Reynolds number on figure 14. In this plot, the value of the decay coefficient corresponding to the rough wooden rod results of Uberoi & Wallis (1967) is not presented. This is due to the fact, as pointed out in the discussion of figure 12, that the increased grid rod roughness leads to an increase in the value of the decay coefficient and the intent in this figure is to compare results for grids made from rods with smooth surfaces.

For $\sigma = 0.34$, and a fixed value of Re_{M_u}, the decay coefficient increases with increasing M_u. The increase is small but not negligible. For example at $Re_{M_u} = 10000$, the increase in mesh size from 2.54 to 5.08 cm leads to about a 15% increase in A.

For both values of M_u, the value of the decay coefficient decreases with increasing Reynolds number. A linear least-square fit to the two sets of decay coefficients (for $M_u = 2.54$ and 5.08 cm) indicates that the rate of decrease with increasing Reynolds number for the two mesh sizes is about the same. Again the variation is small but not negligible. For example, at $M_u = 5.08$ cm, an increase in Re_{M_u} from 10000 to 20000 leads to a 6% decrease in A. The variation of the decay coefficient for grids with $\sigma = 0.44$ is less clear and more data are required before a relationship between A, M_u and Re_{M_u} can be established.

The variation of the decay coefficient with Reynolds number, mesh size, solidity, and surface roughness is not surprising and is due to the variation in drag coefficient of the grid.

5. Concluding remarks

The use of an objective method for the determination of the virtual origin and decay coefficient and exponent when applied to results of the present and previous studies leads to a significant reduction in the scatter of those values. In addition the

dependency on initial conditions such as Reynolds number, mesh size, solidity, grid rod shape and surface roughness can be determined. The method consists of three steps:

(i) Development and use of criteria for the selection of data in the region where the flow is nearly homogeneous and isotropic;

(ii) Use of the method of least squares to find values of the virtual origin and decay coefficient and exponent which minimize the root mean square of the difference between corresponding measured and computed values of the turbulent velocity variance; and,

(iii) Use of data in different ranges of downstream positions to find values for the virtual origin and decay exponent which do not vary as a function of downstream position.

This approach is first evaluated for results which are obtained as part of the present study and then applied to other data. For the present data the mesh Reynolds number and mesh size vary, respectively, from 6000 to 14000 and 2.54 to 5.08 cm. The corresponding range for Re_λ is 28–40. For data from all sources used in the study, the mesh Reynolds number varies from 5150 to 68000; the mesh size varies from 1.27 to 5.08 cm; and, solidities are either 0.34 or 0.44. The corresponding overall range of Re_λ is 28–100.

For this range of parameters and using the approach proposed herein, the exponent in the decay power law is found, with two exceptions, to be independent of Reynolds number, mesh size, solidity, grid rod shape and surface roughness for biplane grids. The value for the decay exponent is found to be 1.300 with a root mean square variation of 0.024. The value of the virtual origin is found to be zero and also to be independent of initial conditions. In contrast, and as expected, the decay coefficient is found to be a function of those same initial conditions.

Thus, based on the constancy of the exponent in the power-law decay for the velocity variance, the turbulence downstream of biplane grids, for the range of conditions of the present study, has a universal self-similar behaviour.

The results also suggest that, for a fixed mesh size, the position where the flow become isotropic is proportional to the characteristic time of the large structure and hence increases with Reynolds number.

We would like to acknowledge one of the referees for his comments which initiated our discussion of the velocity skewness, Dr K. N. Helland for his helpful discussions on that same subject, and Professor W. K. George for some stimulating, general discussions concerning the decay law in grid turbulence. In addition, we would like to acknowledge Jin Chung for help in preparing the figures and George Truesdell for help in editing the manuscript.

REFERENCES

Baines, W. D. & Peterson, E. G. 1951 *Trans. ASME* **73**, 467.

Batchelor, G. K. & Townsend, A. A. 1947 *Proc. R. Soc. Lond.* A **191**, 534.

Batchelor, G. K. & Townsend, A. A. 1948 *Proc. R. Soc. Lond.* A **193**, 539.

Batchelor, G. K. 1953 *The Theory of Homogeneous Turbulence*. Cambridge University Press.

Bennett, J. C. & Corrsin, S. 1978 *Phys. Fluids* **21**, 2129.

Comte-Bellot, G. & Corrsin, S. 1966 *J. Fluid Mech.* **25**, 657.

Comte-Bellot, G. & Corrsin, S. 1971 *J. Fluid Mech.* **48**, 273.

Corrsin, S. 1963 *Encyclopedia of Physics*, vol. 8, part 2, p. 568. Springer.

FRENKIEL, F. & KLEBANOFF, P. S. 1971 *J. Fluid Mech.* **48**, 183.

GEORGE, W. K. 1988 The decay of homogeneous turbulence. In *Transport Phenomena in Turbulent Flows* (ed. M. Hirata & N. Kasagi), p. 1. Hemisphere.

GRANT, H. L. & NISBET, I. C. 1957 *J. Fluid Mech.* **2**, 263.

HELLAND, K. N. & STEGEN, G. R. 1970 *Phys. Fluids* **13**, 2925.

HINZE, J. O. 1959 *Turbulence*. McGraw-Hill.

KÁRMÁN, T. VON & HOWARTH, L. 1938 *Proc. R. Soc. Lond.* A **164**, 192.

KOLMOGOROV, A. N. 1941 *Dokl. Akad. Nauk. SSSR* **31**, 538.

MCCOMB, W. D., SHANMUGASUNDARAM, V. & HUTCHINSON, P. 1990 *J. Fluid Mech.* **208**, 91.

MAXEY, M. R. 1987 *Phys. Fluids* **30**, 935.

MONIN, A. S. & YAGLOM, A. M. 1975 *Statistical Fluid Mechanics*, vol. 2 (ed. J. L. Lumley), p. 113. MIT Press.

PORTFORS, E. A. & KEFFER, J. F. 1969 *Phys. Fluids* **12**, 1519.

SAFFMAN, P. G. 1967 *J. Fluid Mech.* **27**, 581.

SIRIVAT, A. & WARHAFT, Z. 1983 *J. Fluid Mech.* **128**, 323.

SREENIVASAN, K., TAVOULARIS, S. & CORRSIN, S. 1980 *J. Fluid Mech.* **100**, 597.

STEWART, R. W. & TOWNSEND, A. A. 1951 *Phil. Trans. R. Soc. Lond.* A **243**, 141.

STEWART, R. W. & TOWNSEND, A. A. 1951 *Phil. Trans. R. Soc. Lond.* A **243**, 359.

TAYLOR, G. I. 1935 *Proc. R. Soc. Lond.* A **151**, 421.

TENNEKES, H. & LUMLEY, J. L. 1989 *A First Course in Turbulence*, p. 72. MIT Press.

UBEROI, M. S. 1963 *Phys. Fluids* **6**, 1048.

UBEROI, M. S. & WALLIS, S. 1967 *Phys. Fluids* **10**, 1216.

UBEROI, M. S. & WALLIS, S. 1969 *Phys. Fluids* **12**, 1355.

VAN ATTA, C. W. & CHEN, W. 1969 *J. Fluid Mech.* **38**, 743.

WYATT, L. A. 1955 Energy and spectra in decaying homogeneous turbulence. PhD thesis, University of Manchester.